**Rare Metal Materials and Engineering**
Volume 49, Issue 5, May 2020
Available online at www.rmme.ac.cn

Science Press

**Cite this article as:** Rare Metal Materials and Engineering, 2020, 49(5): 1503-1511.

ARTICLE

# Influence of Heat Treatment on Microstructure Evolution and Mechanical Properties of GWZK94 Alloys

**Zhu Jiaxuan[1], Yan Zhaoming[1], Zhang Zhimin[1], Zhang Guanshi[1], Pan Yutian[1], Zhang Long[2]**

*[1] North University of China, Taiyuan 030051, China; [2] Hubei Jiangshan Heavy Industries Co., Ltd, Xiangyang 441057, China*

**Abstract:** In order to eliminate the inhomogeneous structure of as-cast GWZK94 alloys, the homogenization was conducted by resistance heating furnace at 505~520 °C for 8~20 h. Optical microscope (OM), differential scanning calorimeter (DSC), X-ray diffraction (XRD), scanning electron microscope (SEM), energy dispersive spectroscopy (EDS), electron backscatter diffraction (EBSD), universal mechanical tester, and Vickers hardness tester were used to investigate the microstructure evolution and mechanical properties. The results show that the as-cast alloy mainly consists of dendritic $\alpha$-Mg matrix, lamellae with metastable stacking faults (SFs), eutectic phase $Mg_{24}(Gd, Y, Zn)_5$, block-shaped long-period stacking ordered (LPSO) phases $Mg_{12}(Gd, Y)Zn$, and a few RE-rich phases. During the homogenization, the lamellae and $Mg_{24}(Gd, Y, Zn)_5$ eutectic phases gradually dissolve into the matrix, and the volume fraction of block-shaped LPSO phases decreases while the lamellar-shaped LPSO phases grow into grains steadily, and some precipitated particles form near the grain boundaries. At 520 °C, triangle-shaped remelted eutectic phases appear, which indicate the over burning of magnesium alloy. Ultimate tensile strength (UTS), tensile yield strength (YS) and fracture elongation show a tendency corresponding to microstructure evolution, and more uniform hardness is obtained. The homogenization condition is optimized to 515 °C/16 h.

**Key words:** GWZK94 alloys; homogenization; LPSO; microstructure; mechanical properties

Rare earth (RE) elements have incomparable properties because of their particular electronic arrangement [1, 2]. The addition of RE elements in magnesium alloys can not only purify grain boundaries, but also enhance the strength and improve the corrosion resistance [3-5]. However, RE magnesium alloys are mainly used in aerospace and high-tech fields due to the high cost of RE [6]. Adding non-rare earth elements can not only reduce the price, but also generate new second phases [7]. Recently, Mg-RE-Zn alloys, which contain long period stacking order (LPSO) phases, have attracted much attention due to excellent mechanical performance [8-10]. $Mg_{97}Y_2Zn_1$ Mg alloys were fabricated by rapid solidified powder metallurgy by Kawamura et al [11], and their yield strength reaches 610 MPa after extrusion at room temperature, and the microstructure investigation indicated that the addition of Zn results in the appearance of LPSO phases which can hinder the sliding of dislocation and strengthen the matrix.

In fact, as-cast magnesium alloys are rarely used, even though RE magnesium alloys have superior properties [12]. Component segregation and shrinkage defects are unavoidable after solidification [13]. So, further homogenization is needed to eliminate the dendrite segregation of the as-cast structure and to harmonize the volume fraction and distribution of second phases before plastic deformation [14]. Finally, the properties of the alloys are strengthened. Tan et al [15] investigated the effect of homogenization on the enhancement of failure strength of $MgY_{1.06}Zn_{0.76}Al_{0.42}$ alloy, and found that block 14H-LPSO phases are broken into fine platelets with the increase of homogenization time, and the tensile strength and yield strength are improved to 416 and 376 MPa after

Received date: May 12, 2019
Foundation item: Natural Science Foundation of Shanxi Province (201801D121106)
Corresponding author: Pan Yutian, Ph. D., Professor, College of Mechatronics Engineering, North University of China, Taiyuan 030051, P. R. China, Tel: 0086-351-3920566, E-mail: panyutiannuc@163.com

homogenization. Shi et al [12] conducted experiments on homogenization of Mg-13Gd-4Y-2Zn-0.6Zr magnesium alloy. Their results indicated that the homogenization at 500 °C for 24 h can improve the homogeneity of second phases and the elongation of specimens, and (Mg, Zn)$_{24}$(Y, Gd)$_5$ eutectic phases dissolve and Mg$_{12}$(Y, Gd)Zn changes from block-shaped to lamellar-shaped with the increase of homogenization temperature. Therefore, it is beneficial to homogenize magnesium alloys to improve their microstructure and mechanical properties.

Up to now, few researches have concentrated on the homogenization of GWZK94 alloys. Therefore, it is interesting to study the optimal homogenization condition before plastic deformation. In the present study, the as-cast GWZK94 specimens were homogenized at 505~520 °C for 8~20 h. The microstructure evolution and hardness variation were then investigated. Finally, the optimal homogenization condition was achieved.

## 1 Experiment

### 1.1 Materials preparation

The GWZK94 alloy (480 mm in diameter and 2040 mm in length) with a nominal composition of Mg-9Gd-4Y-2Zn-0.5Zr (at%) was fabricated by semi-continuous casting using commercial pure Mg (> 99.9%) and Zn, Mg-30Gd (at%), Mg-30Y (wt%) and Mg-25Zr (wt%) master alloys in an electrical resistance furnace under the atmosphere of $CO_2$ and SF6 with the ratio of 100:1. The actual chemical composition of the alloy is shown in Table 1. Cubic specimens with dimensions of 20 mm×20 mm×40 mm were wire cut from the center of GWZK94 alloy ingot. Then, they were subjected to solid solution treatment.

### 1.2 Homogenization treatment

Homogenization temperatures for heating GWZK94 alloy were determined by differential scanning calorimetry (DSC) analysis on a universal V4.4 DTA DSC instrument. The DSC curve is illustrated in Fig.1. It was obtained by increasing the heating temperature from room temperature to 600 °C at the rate of 10 °C/min, and the curve is shown between 100 °C and 600 °C to highlight the phase transformation. It can be seen that the curve shows a peak at 520 °C, which is the highest temperature allowed for homogenization, or the alloy will undergo phase transformation. Fig.1 shows that the melting point is 588 °C, and four temperatures of 505, 510, 515, and 520 °C are selected according to the homogenization empirical equation $T$=(0.9~0.95)$T_m$. Meanwhile, in order to investigate the microstructure evolution, the heating time was chosen as 8~20 h. After the homogenization, ~70 °C water quenching was performed to prevent the precipitation of supersaturated solid solution in the process of sudden temperature change.

**Table 1 Chemical composition of as-cast GWZK94 alloy (at%)**

| Gd | Y | Zn | Zr | Mg |
|---|---|---|---|---|
| 9.40 | 3.62 | 1.84 | 0.52 | Bal. |

### 1.3 Characterization

Optical microscope (OM, A2m, Zeiss, Oberkochen, Germany) was employed to observe the microstructure with the magnification of 50~500x after the specimens were ground, polished and corroded with picric acid reagent in a solution of 2 mL deionized water, 2 mL 99% acetic acid, 1 g picric acid and 14 mL ethanol. X-ray diffraction (XRD, DX-2700, Fangyuan Inc., Dandong, China) equipped with Cu radiation was applied to identify the phase composition of magnesium alloy with the diffraction angle from 20° to 80° at the speed of 5°/min. Scanning electron microscope (SEM, SU5000, Hitachi, Tokyo, Japan) was used to observe the change of secondary phases during homogenization in different conditions and the phase atomic ratio was defined by energy dispersive spectroscopy (EDS, Genesis, EDAX Inc., Mahwah, NJ, USA) with the voltage of 20 kV and working distance of 10 mm. At last, electron backscatter diffraction (EBSD, EDAX Inc., Mahwah, NJ, USA) were used to determine the grain orientation and intensities of (0001) pole figures with title angle of 70° and working distance of 15 mm. The tensile strength test was carried out on an Instron 3382 universal material testing machine and the hardness was determined by UHL VMHT Vickers hardness tester.

## 2 Results and Discussion

### 2.1 Microstructure of as-cast alloy

From Fig.1, it can be observed that the eutectic transformation temperature and melting temperature are estimated to be 521 and 588 °C, respectively. It can be known that $\alpha$-Mg phases nucleate when the casting cooling temperature decreases to 588 °C, and Zr-rich area may be the nucleation attachment station. Then, the liquid phases and $\alpha$-Mg matrix coexist in the alloy until 521 °C. The addition of 0.5 wt% Zr can help to refine the primary $\alpha$-Mg grains.

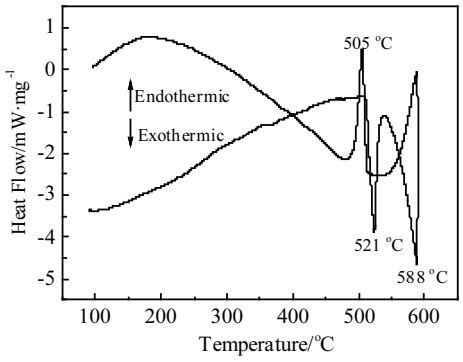


Fig.1 DSC curves of GWZK94 alloy

The eutectic reaction happens when the temperature decreases to about 521 °C. And the reaction equation is shown as follows: L→$\alpha$-Mg+$\beta$-eutectic.

According to the phase transformation process in the phase diagram of the alloy, it can be obtained that the formation of $\alpha$-Mg primary is ahead of $\alpha$-Mg matrix, and some $\alpha$-Mg forms around the eutectic phases with the coexistence of $\alpha$-Mg and eutectic phases.

Fig.2 depicts the microstructure of as-cast GWZK94 alloy. It can be seen that the alloy is mainly composed of $\alpha$-Mg, interdendritic block-shaped phases and intragranular lamellae phases with the average grain size of 84 μm. The interdendritic block-shaped phases are elongated along the grain boundaries with two different contrasts, i.e., bright white and dark grey, which are marked as points E and F, respectively; bright white phase in square shape is marked as G as shown in Fig.2d. The intragranular lamellae in the $\alpha$-Mg matrix is stretched through the whole grain with special orientation, while some grains have no existence of lamellae structure due to no existence of eutectic phases at the grain boundaries like the grains at the top of Fig.2d. Ding et al[16] investigated that the lamellae structure in $\alpha$-Mg matrix of as-cast $Mg_{96.32}Gd_{2.5}Zn_1Zr_{0.8}$ alloy is stacking faults (SFs) with a distinctive 14H-type LPSO structure. Meanwhile, the investigation of Wu et al [17] also confirmed this. Specifically, the SFs form because the interaction of Mg, Gd, Y and Zn atoms influences the normal lattice location. When the thermodynamic and dynamic conditions are prepared for elemental composition and stacking order of Y and Zn or Gd and Zn, the lamellae forms in the Mg matrix. But not all grains have the lamellae structure because Gd, Y and Zn atoms are mainly composed of the eutectic phases, around which the grains are easy to form the lamellae[16, 17].

In order to identify the composition of eutectic phases, EDS analysis was conducted on the secondary phases. Table 2 shows the chemical composition of phases in GWZK94 alloy shown in Fig.2d. The results indicate that phase E is composed of Mg-11.87Gd-3.74Y-2.02Zn (at%), while phase F consists of Mg-4.41Gd-2.84Y-5.37Zn (at%). LPSO and $Mg_{24}(Gd, Y, Zn)_5$ are detected in the as-cast alloy by XRD (Fig.3). The ratio of (Gd+Y):Zn in phase F is 1.08, similar to the ratio of 1.0 for $Mg_{12}(Gd, Y)Zn$ which is a kind of 14H-LPSO structure [18]. The ratio of Mg:(Gd+Y+Zn) for phase E is 4.6, similar to the ratio of 4.8 for $Mg_{24}(Gd, Y, Zn)_5$. Meanwhile, the acceptable errors are inevitable. The lamellae structure shown in Fig.2d is also detected in Mg-6.9Gd-3.2Y-1.5Zn-0.5Zr alloy by Zhou et al [19]. It is found that the lamellae structure is a kind of metastable/imperfect LPSO structure or SFs, and such LPSO structure might be transformed into a stable structure during homogenization[16, 17, 20]. The content of Gd and Zn is very small according to the analysis of EDS. Thus, the lamellae structure might be a kind of unstable SFs. Finally, the square shape bright white phase marked as G in Fig.2d has a high content of RE elements, which can be defined as RE-rich phase [21]. The similar result is also obtained by Ding et al[16], but the chemical composition of the square-shaped phase is different. Li et al[22] indicated that the square-shaped phases have the same fcc crystal structure but the composition is various for the reason of different alloy types. Meanwhile, Wu et al[23] reported that square-shaped phases are relatively stable and

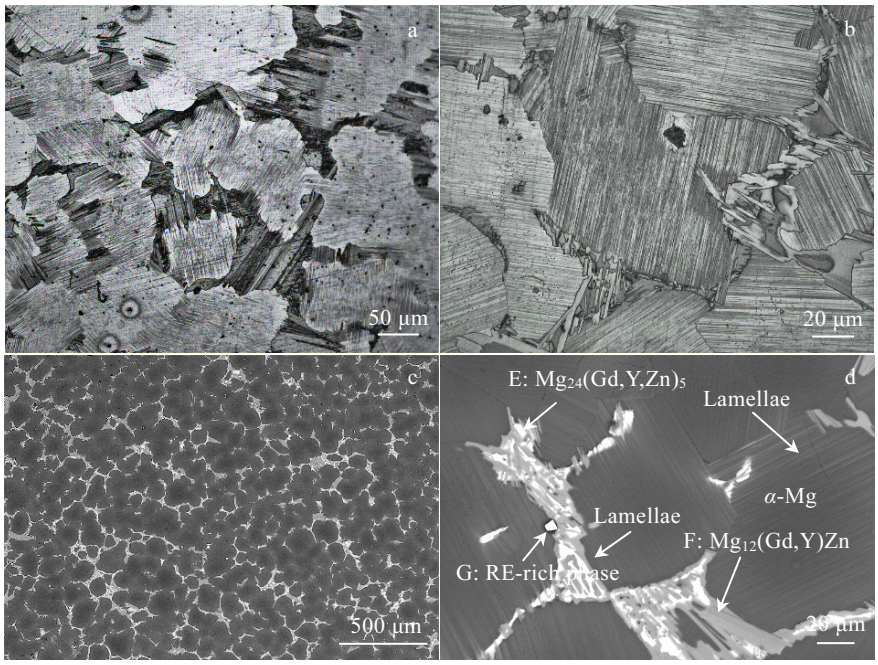


Fig.2 OM images (a, b) and backscattered electron (BSE) images (c, d) of as-cast GWZK94 magnesium alloy

**Table 2 EDS results of marked points of GWZK94 alloy shown in Fig.2d (at%)**

| Point | Gd | Y | Zn | Zr | Mg |
|---|---|---|---|---|---|
| E | 11.87 | 3.74 | 2.02 | 0.41 | 81.95 |
| F | 4.41 | 2.84 | 5.37 | 0.38 | 87.00 |
| G | 35.38 | 50.73 | 1.17 | 4.17 | 11.55 |
| Lamellae | 1.77 | 0.82 | 0.21 | 0.22 | 96.98 |

the chemical composition cannot be changed during the heat treatment. Moreover, it can be seen that the content of Y is higher than that of Gd, which can be attributed to the nucleation condition of RE-rich phases, and the same result is achieved for Mg-7Y-4Gd-1Zn alloys[24]. Several studies[16, 17, 23, 25, 26] have reported that a small amount of RE-rich phases are formed in as-cast Mg-RE(-Zn) alloys and abundant after high-temperature treatment. In GWZK94 alloys, the formation of RE-rich phases can be attributed to the extra Gd and Y elements after the formation of eutectic and LPSO phases during the solidification of as-cast alloys segregated and nucleated near the boundaries. From the TEM observation of Li et al[22], the shape of the square-shaped phase is regular and it seems to grow from the matrix.

Fig.4 illustrates the SEM images and distribution of solute elements in the as-cast GWZK94 alloy. It can be seen that Mg element is mainly distributed in the matrix and a few element is distributed in eutectic phases. Gd occupies bright white phases ($Mg_{24}$(Gd, Y, Zn)$_5$) in the interdendritic block-shaped phases, and Zn is the important element to form the grey phases (interdendritic LPSO phases). Furthermore, the distribution of elements Y and Zr is dispersed. To eliminate segregation and to improve the formability of as-cast alloy, optimal homogenization parameters must be ensured.

## 2.2 Microstructure evolution of homogenized alloys

Fig.5 demonstrates the homogenized microstructures of GWZK94 alloy at 510 °C for different holding time. In general, it can be seen that the volume fraction of network eutectic phases at grain boundaries in as-cast alloy decreases with the increase of holding time. To be specific, coarse eutectic phases dissolve into the matrix and form the supersaturated solid solution. When homogenization time is 8 h (Fig.5a), a tiny change can be observed that lamellae structure in the $\alpha$-Mg matrix dissolves due to its metastable/imperfect structures. The bright white phases $Mg_{24}$(Gd, Y, Zn)$_5$ in eutectic phases dissolve mostly, while grey phases (interdendritic block-shaped LPSO phases) dissolve partly. Meanwhile, fine granular phases precipitated near the boundaries can be observed, which might be the precipitation of supersaturated $\alpha$-Mg matrix or the decomposition of eutectic phases [27]. With increasing the holding time to 12 h (Fig.5b), a dramatic change happens that metastable lamellae phases dissolved into the Mg matrix, making the center grains smooth, and distinct straight lamellar-shaped phases are generated at grain boundaries[16, 17, 19, 23, 28, 29]. The volume fraction of

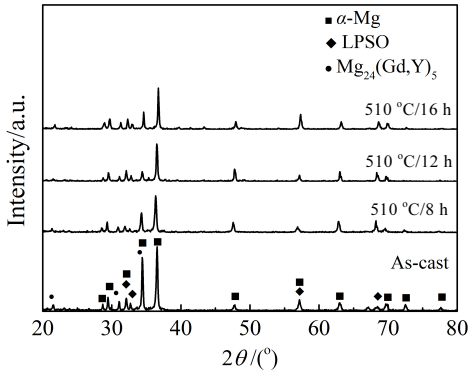


Fig.3 XRD patterns of GWZK94 alloy at 510 °C for different homogenization time

eutectic phases is further reduced compared to holding for 8 h. Meanwhile, new kinds of fine lamellar-shaped phases are obtained which grow from block-shaped LPSO phases at the grain boundaries to intragranular region. This phenomenon has been reported by Li et al, and the lamellar-shaped phases are defined as 14H-LPSO phases [22]. SEM image of holding for 16 h (Fig.5c) indicates the further reduction of eutectic phases. Meanwhile, some precipitated phases are distributed in the matrix irregularly and more precipitated phases near the boundaries are formed. Specifically, with the increase of holding time, supersaturated solid solution forms, and block-shaped LPSO phases at grain boundaries dissolve and transform to lamellar-shaped LPSO phases with the precipitation of supersaturated phases. Some researchers suggested that the formation of LPSO phases depends on the ratio of RE/Zn, and $Zn_6RE_8$ (at%) is an ideal ABCA stacking structure 18R and 14H face-centered cubic (fcc) structure [28]. Thus, the solid solubility of Gd and Y elements increases gradually in the matrix with the increase of homogenization time, corresponding to the growth of lamellar-shaped LPSO phases. However, as the homogenization time increases to 20 h (Fig.5d), no significant effect is observed, which might be the reduction of the solute concentration gradient during the treatment. In other words, early stage homogenization treatment has a more significant effect on the transformation of secondary phases. Meanwhile, the area fraction of lamellar-shaped LPSO phases shows a trend of reduction, which might be the supersaturation of Gd in the matrix. Some studies investigated that the binding ability between Gd and Zn in the matrix is weaker than that between Y and

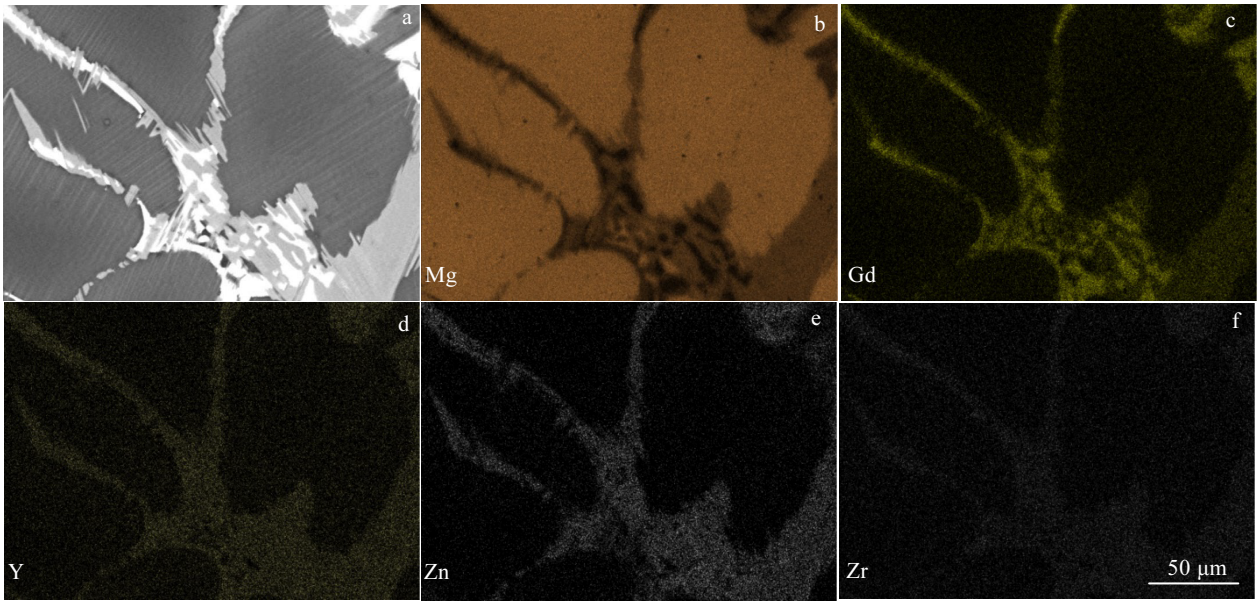


Fig.4 SEM image (a) and distribution of the solute elements in the as-cast GWZK94 alloy: (b) Mg, (c) Gd, (d) Y, (e) Zn, and (f) Zr

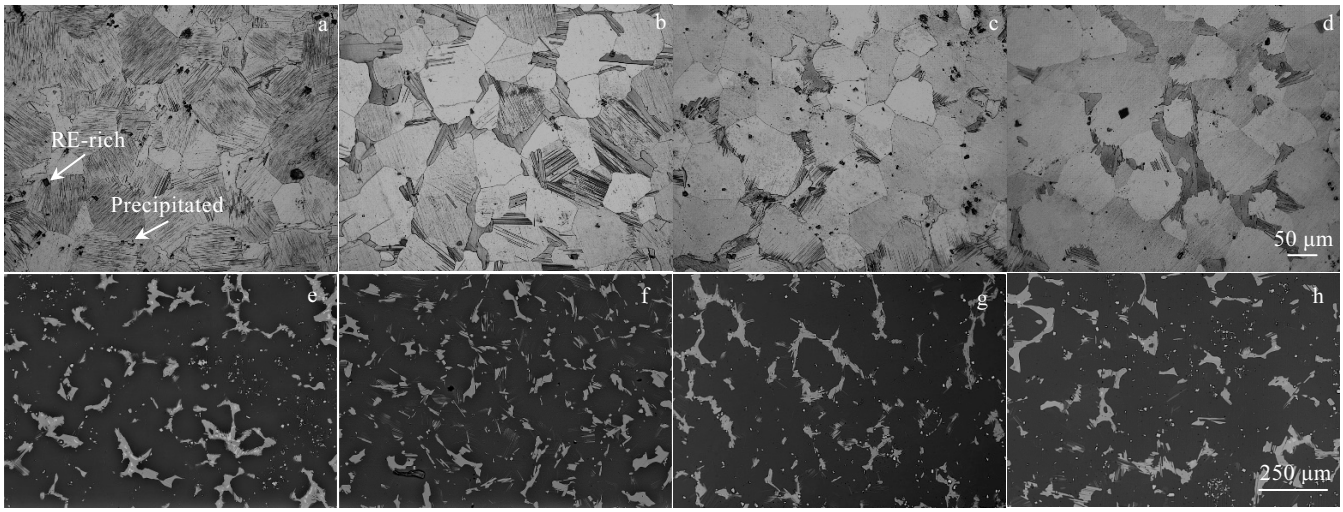


Fig.5 OM (a~d) and SEM (e~h) images of GWZK94 alloy at 510 °C for different homogenization time: (a, e) 8 h, (b, f) 12 h, (c, g) 16 h, and (d, h) 20 h

Zn, and excessive Gd inhibits the transformation of LPSO phases. The stable fine lamellar-shaped 14H-LPSO structure is beneficial to deformation, which is attributed to its kink deformation[30].

Fig.6 illustrates the microstructure evolution of homogenized samples at different temperatures for 16 h. In general, network coarse eutectic phases in the as-cast alloy dissolve greatly and form the discontinuous eutectic compounds. Meanwhile, metastable SFs dissolve and lamellar-shaped LPSO forms. Some phases with irregular shape are precipitated near the boundaries. At 505 °C (Fig.6a), there is also a little bit of $Mg_{24}(Gd, Y, Zn)_5$ phases mixed in block-shaped LPSO phases, which indicates incomplete homogenization. Some eutectic phases still maintain the network shape. With increasing the temperature up to 510 and 515 °C (Fig.6b and 6c), the bright white $Mg_{24}(Gd, Y, Zn)_5$ phases dissolve completely, and the volume fraction of secondary phases decreases to 12% and 10.8% from as-cast 15%. At the same time, it is worth noting that square-shaped RE-rich phases are difficult to dissolve at high temperatures and show an increasing number fraction. Gao et al [29] found that the square-shaped RE-rich phases are stable and pin the grain boundaries, making the Mg-Gd-Y-Zr alloys less sensitive to high temperature and improving the

mechanical properties. Furthermore, they thought that the formation of square-shaped phases in heat treatment is determined by the transformation in the dissolution process of eutectic phases. When the temperature reaches 520 °C (Fig.6d), the remelting of phases appears at the grain boundaries, which indicates the over-burning of alloy. Remelting of eutectic sphere, widening of grain boundaries and remelting of triangular grain boundaries are three characteristics for identifying the over-burning of alloy [13]. Fig.6i shows the high magnification of Fig.6h, and the remelting of triangular phases can be seen obviously. The distribution of Gd, Y, Zn and Zr elements after homogenization treatment at 515 °C for 16 h is shown in Fig.6j. It can be seen that the uniform distribution of elements is observed under 515 °C/16 h. To be specific, enrichment of Gd and Zn elements in interdendritic eutectic eliminates the segregation after the dissolution of eutectic compound. Above all, 515 °C/16 h is the optimum homogenization condition.

Fig.7 shows the schematic diagram of microstructure evolution during the homogenization. The $\alpha$-Mg with metastable SFs is surrounded by network eutectic phases. Furthermore, square-shaped RE-rich phases are distributed in the matrix. At the initial stage of homogenization, part of metastable SFs dissolve in the matrix and transform into stable intragranular LPSO phases, and $Mg_{24}(Gd, Y, Zn)_5$ in eutectic phases at the boundaries begins to dissolve, corresponding to the strengthening of solid solution. Also, there is no significant growth in the grain size. It is noticed that limited fraction of precipitated phases near the boundaries can be observed. Under the condition of 515 °C/16 h which is the optimum condition of homogenization, $Mg_{24}(Gd, Y, Zn)_5$ dissolves completely and the volume fraction of interdendritic LPSO phases decreases from 15% to 10.8%, corresponding to the increase of intragranular LPSO phases. The RE-rich phases are almost unchanged, which indicates the feature of high temperature insolubility. Furthermore, an increased number of precipitated phases can be obtained during the homogenization, which is due to the supersaturation of the matrix or the decomposition of secondary phases. Eventually, a relatively homogeneous structure is obtained under the condition of 515 °C/16 h.

### 2.3 Mechanical properties

To analyze the effect of homogenization on the anisotropy of GWZK94 alloy, the texture of as-cast and homogenized alloy is examined by electron back-scattered diffraction (EBSD) and the results are illustrated in Fig.8. Different colors of different grains shown in Fig.8a and 8b

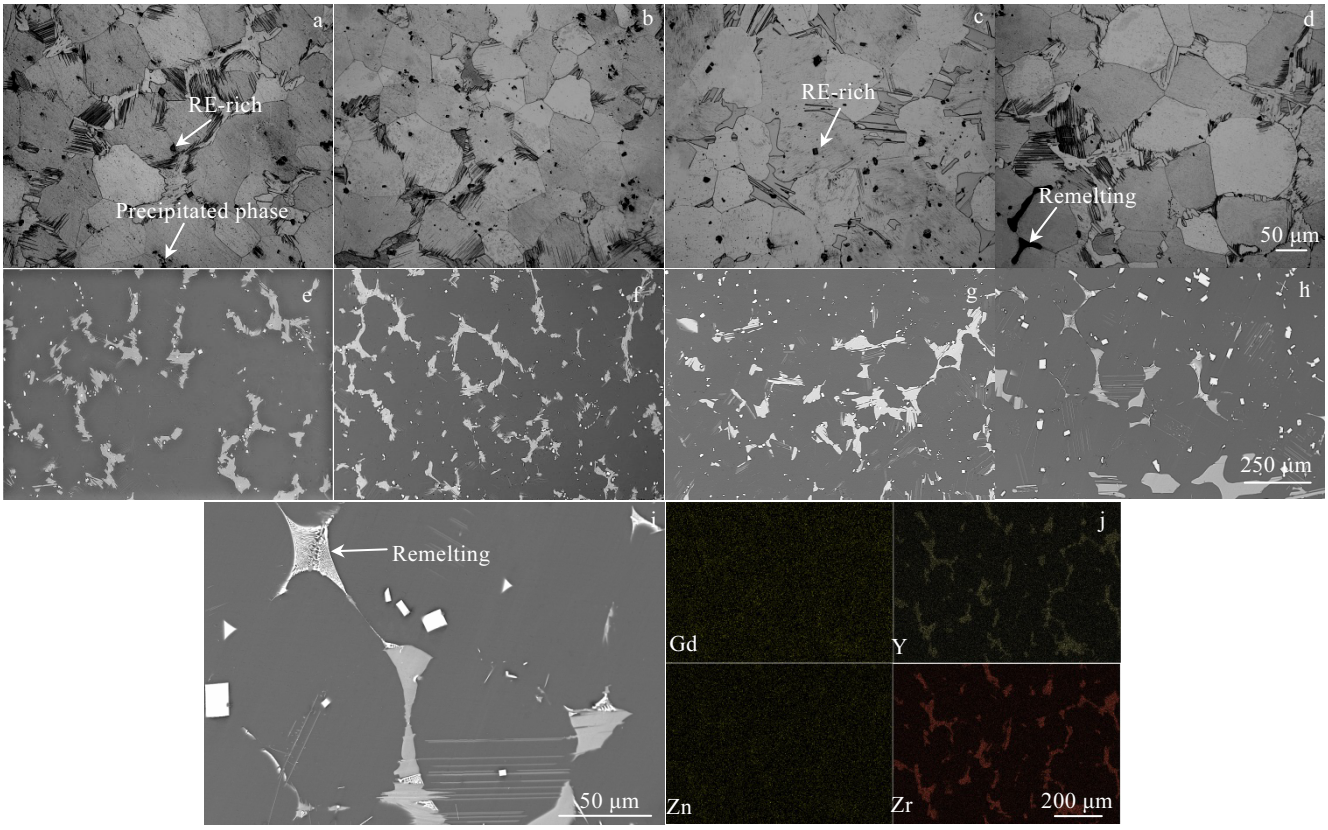


Fig.6 OM (a~d) and SEM (e~i) images of microstructure evolution of GWZK94 alloy homogenized at different temperatures for16 h: (a, e) 505 °C, (b, f) 510 °C, (c, g) 515 °C, and (d, h) 520 °C; high magnification of Fig.6h (i); distribution of solute elements in homogenized alloy at 515 °C/16 h (j)

illustrate different grain orientation, and the black region represents the eutectic phases, corresponding to the EBSD confidence index (CI) less than 0.1 which cannot be distinguished by the system. As shown in Fig.8a and 8b, it can be noted that the volume fraction of interdendritic eutectic phases dramatically decreases after the homogenization treatment. Meanwhile, the grain size increases slightly from 92 μm to 106 μm, which is attributed to the increase of grain boundary energy and migration provided by the high temperature and holding time. Fig.8c and 8d show the texture in (0001) level of as-cast and homogenized alloy, respectively. It can be seen that the alloy exhibits random texture with random orientation. Thus, the anisotropy of as-cast and homogenized alloy does not exist. Therefore, the mechanical properties are not related to the direction of cutting materials.

The mechanical properties of the as-cast and homogenized samples measured at room temperature are demonstrated in Fig.9. It can be observed from Fig.9a that the ultimate tensile strength (UTS) increases from 197.1 MPa to 218.4 MPa after 515 °C/16 h homogenization, while the tensile yield strength (TYS) decreases from 143.2 MPa to 130.4 MPa. It is obviously known the obstacle of precipitated

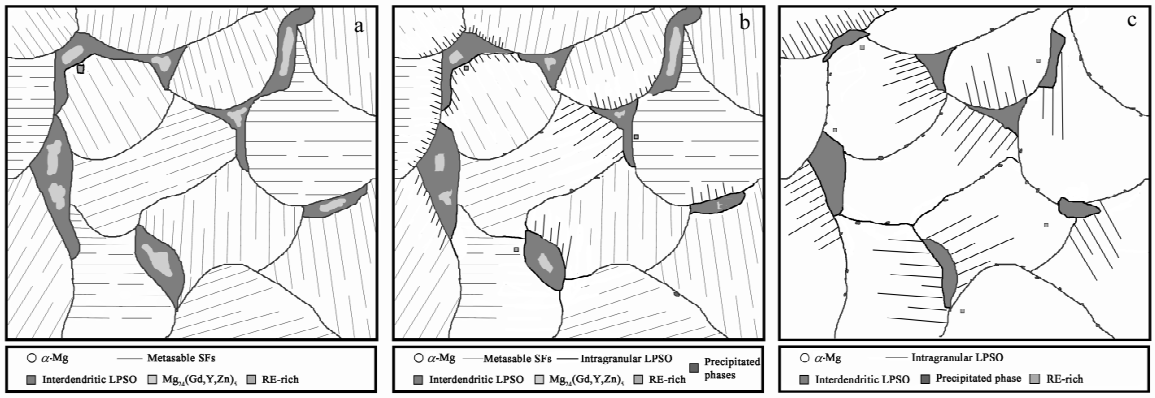


Fig.7 Schematic diagram of microstructure evolution of GWZK94 alloy during homogenization: (a) initial structure, (b) microstructure during homogenization, and (c) homogenized under 515 °C /16 h

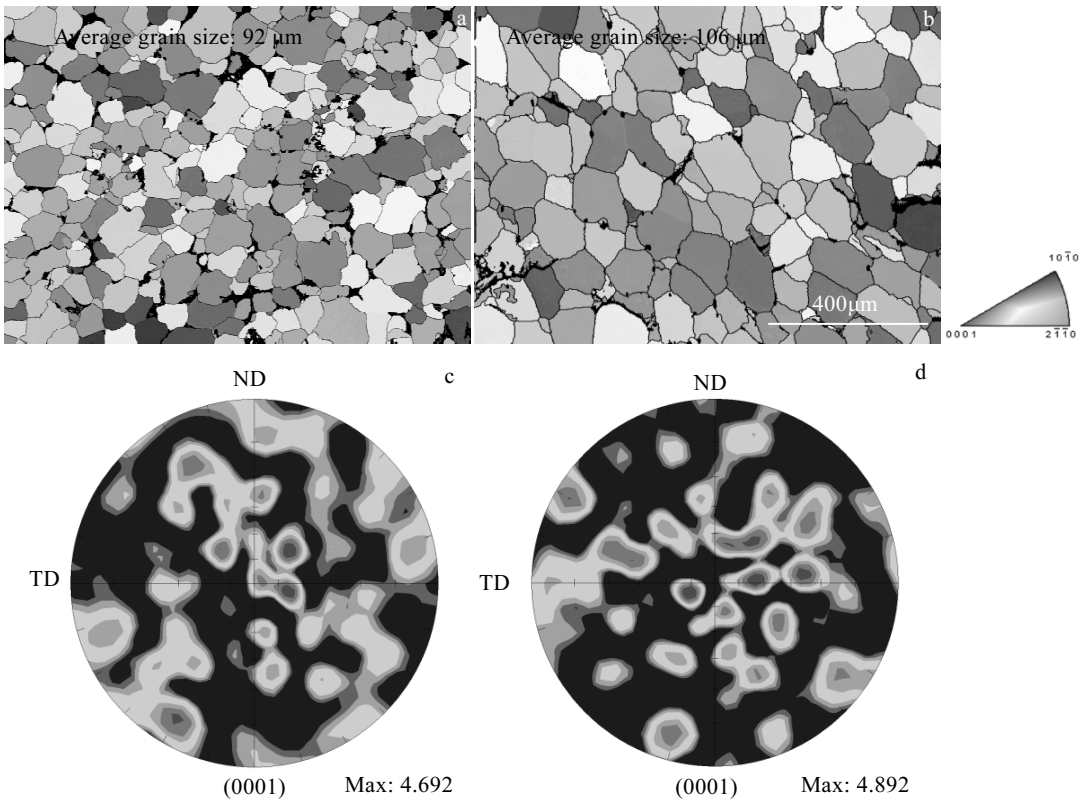


Fig.8 Grain orientation and IPF (a, b); (0001) pole figures (c, d) of GWZK94 alloy: (a, c) as-cast and (b, d) homogenized under 515 °C/16 h

phases to the slip of dislocation can strengthen the matrix, which causes the increase of UTS. Besides, the TYS is primarily influenced by three common factors which are grain size, solid solution strengthening and secondary phases [31]. To be specific, at the initial stage of homogenization treatment, the secondary phases dissolve into the matrix, resulting in lattice distortion and solid solution strengthening. Also, the grain growth is not obvious, and the precipitation of secondary phases at the boundaries hinders the motion of dislocation. Thus, the TYS increases in the early stage. However, with the increase of temperature and holding time (16 h or more), the formation of precipitates at the boundaries consumes part of solutes in the matrix, so solid solution strengthening becomes weak and the coarsening of grain plays a leading role. Therefore, TYS decreases after homogenization under 515 °C/16 h compared to that of as-cast alloy. In addition, the elongation (El) of samples increases from 4.1% to 5.3% after homogenization. As described, the dissolution of secondary phases after homogenization releases the inner strain and eliminates the segregation, corresponding to the reduction of crack tendency during deformation.

It is believed that the microhardness is influenced by the microstructure evolution to a certain extent. Fig.9b shows the Vickers hardness change of as-cast and homogenized (515 °C/16 h) samples. Ten points of the as-cast and homogenized alloys are tested and the selected positions are shown in the upper left corner of Fig.9b. A significant non-uniform performance is observed in the black line shown in Fig.9b, which is due to the existence of composition segregation and nonequilibrium eutectic phases in the as-cast alloy. After homogenization at 515 °C for 16 h, the dispersion of microhardness curve decreases compared with the as-cast curve, which is shown by the red line. Furthermore, the value of Vickers hardness after homogenization is lower than that in as-cast condition, corresponding to the decrease of tensile strength. The researches of Yuan et al [32] and Singh et al [33] suggest that the solid solution can increase the strength of matrix, and the coarsening of grains can reduce the influence of the solid solution. Meanwhile, the hardness of secondary phases in Mg-RE-Zn alloy is higher than that of the matrix. In the present work, under the condition of 515 °C/16 h, the coarsening of grains plays a leading role in reducing the microhardness, which can also explain the decrease of tensile strength. Furthermore, uniform distribution of microhardness also indicates the homogeneous composition and elimination of segregation after homogenization under 515 °C/16 h.

/

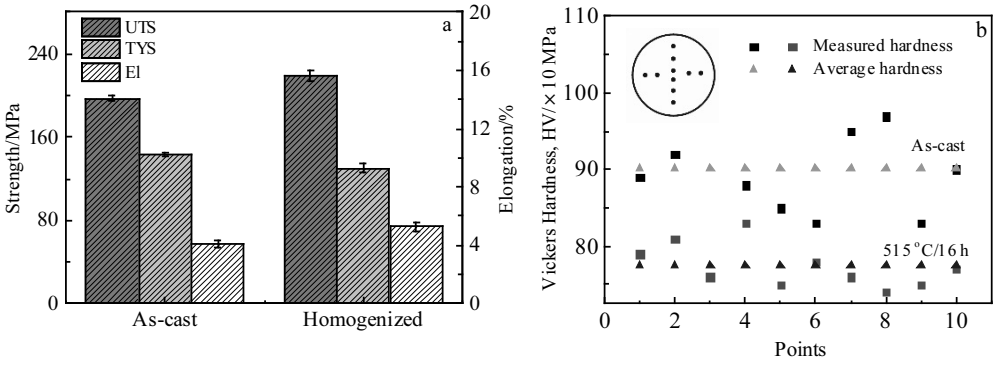


Fig.9 Mechanical properties of as-cast and homogenized (515 °C/16 h) alloy measured at room temperature: (a) tensile properties and (b) Vickers hardness

## 3 Conclusions

1) The as-cast alloy mainly consists of dendritic $\alpha$-Mg matrix, lamellae composed of metastable SFs attached in $\alpha$-Mg, network eutectic compounds ($Mg_{12}$(Gd,Y)Zn, $Mg_{24}$(Gd, Y, Zn)$_5$) distributed along grain boundaries, and RE-rich phases with square shape. Serious element segregation exists in the as-cast alloy, corresponding to the distribution of Gd and Zn along interdendritic phases.

2) The optimal homogenization condition is determined to be 515 °C/16 h. After homogenization, lamellae with metastable SFs within $\alpha$-Mg dissolves, and the area fraction of interdendritic eutectic compounds decreases to 10.8%, corresponding to $Mg_{24}$(Gd, Y, Zn)$_5$ which is transformed into interdendritic block-shaped $Mg_{12}$(Gd,Y)Zn. Meanwhile, lamellar-shaped LPSO phases grow from grain boundary to grain interior, and some participated phases are gathered near the boundaries irregularly.

3) After homogenization, the mechanical properties change to various degrees. One the hand, the ultimate tensile strength (UTS) increases from 197.1 MPa to 218.4 MPa owing to the obstacle of precipitated phases to the slip of dislocation, while the tensile yield strength (TYS) decreases from 143.2 MPa to 130.4 MPa as a result of coarsening of grains. One the other hand, the elimination of inner strain and segregation determine the increase of elongation from 4.1% to 5.3%. Also, the hardness is more uniform and the coarsening of grains decreases the hardness, which is helpful to plastic deformation.

## References


1 Zhou Xiaojie, Liu Chuming, Gao Yonghao *et al. Journal of Materials Engineering and Performance*[J], 2018, 27(11): 6237

2 Yan Zhaoming, Fang Min, Lian Zhendong *et al. Metals*[J], 2019, 9(5): 563

3 Zhang Zhimin, Yan Zhaoming, Du Yue *et al. Materials*[J], 2018, 11(11): 2282

4 Zhang Guanshi, Zhang Zhimin, Li Xubin *et al. Journal of Alloys and Compounds*[J], 2019, 790: 48

5 Du Yue, Zhang Zhimin, Zhang Guanshi *et al. Rare Metal Materials and Engineering*[J], 2018, 47(5): 1422

6 Zhang Guanshi, Zhang Zhimin, Du Yue *et al*. *Materials*[J], 2018, 11(11): 2092

7 Zhang Zhimin, Du Yue, Zhang Guanshi *et al*. *Materials Transaction*[J], 2018, 59(4): 669

8 Zhou Xiaojie, Liu Chuming, Gao Yonghao *et al*. *Materials Characterization*[J], 2018, 135: 76

9 Xu Chao, Nakata Taiki, Qiao Xiaoguang *et al. Scientific Reports*[J], 2017, 7(1): 40 846

10 Liu Xuan, Zhang Zhiqiang, Hu Wenyi *et al*. *Journal of Materials Science & Technology*[J], 2016, 32(4): 313

11 Matsuda M, Ii S, Kawamura Y *et al. Materials Science & Engineering A*[J], 2005, 393: 269

12 Shi Wenjiang, Zhang Zhimin, Meng Mu *et al*. *Materials Research Express*[J], 2018, 5(1): 16 514

13 Xiao Lei, Yang Guanyu, Liu Yang *et al. Journal of Materials Science & Technology*[J], 2018, 34: 2246

14 Zhang Guodong, Li Xinggang, Ma Minlong *et al. Journal of Rare Earth*[J], 2014, 32(5): 445

15 Tan X H, Chee K H W, Chan K W J *et al. Materials Science & Engineering A*[J], 2015, 644(17): 405

16 Ding W J, Wu Y J, Peng L M *et al. Journal of Materials Research*[J], 2009, 24(5): 1842

17 Wu Y J, Lin D L, Zeng X Q *et al. Journal of Materials Science*[J], 2009, 44: 1607

18 Zhu Y M, Morton A J, Nie J F. *Acta Materialia*[J], 2010, 58: 2936

19 Zhou Xiaojie, Liu Chuming, Gao Yonghao *et al*. *Metallurgical and Materials Transactions A*[J], 2017, 48(6): 3060

20 Kim Jin-Kyung, Ko Won-Seok, Sandlobes SandlÖbes *et al. Acta Materialia*[J], 2016, 112(15): 171

21 Yu Jianmin, Zhang Zhimin, Xu Ping *et al. Journal of Alloys and Compounds*[J], 2019, 787: 239

22 Li D J, Zeng X Q, Dong J *et al. Journal of Alloys and Compounds*[J], 2009, 468(1-2): 164

23 Wu Y J, Zeng X Q, Lin D L *et al. Journal of Alloys and Compounds*[J], 2009, 477(1-2): 193

24 Zhang Li, Zhang Jinghai, Xu Chi *et al. Materials & Design*[J], 2014, 61: 168

25 Zhang Li, Zhang Jinghai, Leng Zhe *et al. Materials & Design*[J], 2014, 54: 256

26 Yin D D, Wang Q D, Gao Y *et al. Journal of Alloys and Compounds*[J], 2011, 509(5): 1696

27 Li M, Wang X, Feng Q Y *et al. Materials Characterization*[J], 2017, 125: 123

28 Liu Huan, Bai Jing, Yan L *et al. Materials & Design*[J], 2016, 93(5): 9

29 Gao Yan, Wang Qudong, Gu Jinhai *et al. Materials Science and Engineering A*[J], 2007, 459(1-2): 117

30 Yu Jianmin, Zhang Zhimin, Wang Qiang *et al. Journal of Alloys and Compounds*[J], 2017, 704: 382

31 Wen Kai, Xiong Baoqing, Zhang Yongan *et al*. *Rare Metal Materials and Engineering*[J], 2017, 46(4): 928

32 Yuan Guanyin, Liu Yong, Lu Chen *et al. Materials Science & Engineering A*[J], 2008, 472(1-2): 75

33 Singh Alok, Osawa Yoshiaki, Somekawa H *et al. Scripta Materialia*[J], 2011, 64: 661


# 热处理对 GWZK94 合金微观组织与力学性能的影响


朱家萱[1]，闫钊鸣[1]，张治民[1]，张冠世[1]，潘玉田[1]，张　龙[2]

(1. 中北大学，山西 太原 030051)

(2. 湖北江山重工有限责任公司，湖北 襄阳 441057)



**摘　要**：为了改善铸态 GWZK94 合金微观组织的不均匀性，使用电阻加热炉在温度 505~520 ℃范围内保温 8~20 h 进行热处理实验。采用光学显微镜（OM），差示扫描量热仪（DSC），X 射线衍射仪（XRD），扫描电子显微镜（SEM），能谱仪（EDS），电子背散射衍射技术（EBSD），万能试验机和维氏硬度计进行微观组织演变及力学性能分析。结果表明，铸态合金组织主要包括树枝状 $\alpha$-Mg 基体，含亚稳态层错（SFs）的片层结构，共晶相 $Mg_{24}(Gd, Y, Zn)_5$，块状长周期有序堆垛结构（LPSO, $Mg_{12}(Gd, Y)Zn$）和少量的富稀土相。在均匀化处理过程中，片层结构和共晶相 $Mg_{24}(Gd, Y, Zn)_5$ 逐渐溶于基体中，同时块状 LPSO 相体积分数逐渐减小并伴随有片层状 LPSO 相向晶粒内部生长，颗粒状相在晶界附近析出。加热温度为 520 ℃时出现复熔三角晶界，说明此时发生了合金的过烧现象。经过均匀化处理后，合金的极限抗拉强度（UTS）和拉伸屈服强度（TYS）表现出了与组织演变规律相同的变化趋势，同时得到了较为均匀的硬度分布。最佳的均匀化制度为 515 ℃/16 h。



**关键词**：GWZK94合金；均匀化；LPSO；组织；力学性能



作者简介：朱家萱，女，1991 年生，博士，中北大学机电工程学院，山西 太原 030051，电话：0351-3920566，E-mail: nucjxzhu@126.com